

Narrow resonances studies with the radiative return methodHenryk Czyż,¹ Agnieszka Grzebińska,² and Johann H. Kühn³¹*Institute of Physics, University of Silesia, PL-40007 Katowice, Poland*²*Institute of Nuclear Physics Polish Academy of Sciences, PL-31342 Cracow, Poland*³*Institut für Theoretische Teilchenphysik, Karlsruhe Institute of Technology, D-76128 Karlsruhe, Germany*

(Received 1 February 2010; published 12 May 2010)

Using the radiative return method, experiments at high luminosity electron-positron colliders allow one to explore the kaon and the pion form factors in the timelike region up to fairly high energies. This opens the possibility to study kaon and pion pair production at and around the narrow resonances J/ψ and $\psi(2S)$ and to explore the interference between electromagnetic and hadronic amplitudes. Parametrizations of charged and neutral kaon as well as pion form factors are derived, which lead to an improved description of the data in the region of large invariant masses of the meson pair. These form factors are combined with the hadronic couplings of charged and neutral kaons to J/ψ and $\psi(2S)$ and implemented into the Monte Carlo generator PHOKHARA, which is now, for the first time, able to simulate the production of narrow resonances and their decay into kaon, pion, and muon pairs.

DOI: 10.1103/PhysRevD.81.094014

PACS numbers: 13.66.Bc, 13.20.Gd, 13.25.Gv, 13.40.Gp

I. INTRODUCTION

New and precise measurements of the cross section for electron-positron annihilation into hadrons have been performed during the past years, which were based on the method of “Radiative Return” [1,2]. Exclusive reactions, specifically two-body final states like $\pi^+\pi^-$ [3,4], $p\bar{p}$ [5], or $\Lambda\bar{\Lambda}$ [6] and three- [7,8] and four-meson final states [9,10] have been explored. An important ingredient in these analyses was and is the simulation of all these reactions through a Monte Carlo generator. In the first step, the generator EVA was developed [2,11], which is based on leading order matrix elements combined with structure function methods for an improved treatment of initial state radiation. Subsequently the complete next-to-leading order (NLO) QED corrections were evaluated [12,13] and implemented into the generator PHOKHARA [14–22], which is now available for a variety of exclusive final states. (For a recent review of theoretical and experimental results see e.g. [23].) B -meson factories, operating at energies around 10 GeV and with high luminosity, allow one to explore hadronic final states with relatively large invariant masses, up to 3 GeV and beyond. Therefore, the narrow resonances J/ψ and $\Psi(2S)$ can be studied through the radiative return, in particular, in decay channels of low multiplicity, leptonic ones like $\mu^+\mu^-$ [24], or two-body hadronic modes like $\pi^+\pi^-$, K^+K^- , $K^0\bar{K}^0$, or $p\bar{p}$ [5]. The signal is identified with the help of a very good mass resolution and particle identification in the resonance region.

For an analysis exploiting the large statistics, the inclusion of radiative corrections from initial- and final-state radiation (ISR and FSR) is mandatory, since it affects the cross section and the line shape of the resonance. For the simulation of hadronic final states both the electromagnetic contribution, i.e. a parametrization of the form factor, and

the strength of the direct coupling of the resonance to the hadrons are required. The latter is absent for final states with positive G -parity ($2\pi, 4\pi, \dots$) but nonvanishing e.g. for $K\bar{K}$, 3π , or final states with baryons. On the other hand, a careful analysis of the resonance line shape in the various channels would allow a model-independent determination of the direct coupling and of the form factors close to resonance [25–31].

With this motivation in mind we reanalyze the pion and kaon form factors with emphasis on the region above the ρ resonance. The basic ingredients are very similar to those employed in an earlier study [32]. However, additional assumptions are required to properly describe the different resonancelike structures in the energy region between 1 GeV and 3 GeV. The details of this model and its parameters are described in Secs. II and III for pions and kaons, respectively. The new implementation of these modes into PHOKHARA, which includes, as before, NLO ISR and FSR, is presented in Sec. IV. Section V is concerned with the implementation of the narrow resonances in the channels $\mu^+\mu^-$, $\pi^+\pi^-$, K^+K^- , and $K^0\bar{K}^0$. Hadronically and electromagnetically induced amplitudes are included, together with the radiative corrections from ISR and FSR. Section VI contains a brief summary and our conclusions.

II. THE PION FORM FACTOR

For a realistic generation a model for the electromagnetic form factor is required. The ansatz presented in [32] was published before the CLEO- c measurement of the form factor in the vicinity of the $\psi(2S)$ resonance [33] and underestimates the experimental result significantly. The same applies to the model predictions at J/ψ as compared to the pion form factor calculated in [31] from $B(J/\psi \rightarrow \pi^+\pi^-)$ and $B(J/\psi \rightarrow e^+e^-)$ decay rates.

To accommodate the new data, the updated model ansatz for the pion form factor is taken similarly to [32]

$$F_\pi(s) = \left[\sum_{n=0}^N c_{\rho_n}^\pi \text{BW}_{\rho_n}(s) \right]_{\text{fit}} + \left[\sum_{n=(N+1)}^{\infty} c_{\rho_n}^\pi \text{BW}_{\rho_n}(s) \right]_{d\text{QCD}}, \quad (1)$$

however, with a different set of parameters. Those of the first $N + 1$ ρ radial excitations are fitted and the rest are taken from the ‘‘dual QCD model’’ [34]. It is necessary to take $N = 5$ to fit the data. For the precise treatment of ρ_4 and ρ_5 see below.

For the Breit-Wigner (BW) function we adopt the Gounaris-Sakurai [35] version with pion loop corrections included:

$$\text{BW}_{\rho_n}(s) = \frac{m_{\rho_n}^2 + H(0)}{m_{\rho_n}^2 - s + H(s) - i\sqrt{s}\Gamma_{\rho_n}(s)}, \quad (2)$$

where

$$H(s) = \hat{H}(s) - \hat{H}(m_{\rho_n}^2) - (s - m_{\rho_n}^2) \frac{d}{ds} \hat{H}(m_{\rho_n}^2), \quad (3)$$

$$\hat{H}(s) = \left(\frac{m_{\rho_n}^2 \Gamma_{\rho_n}}{2\pi [p(m_{\rho_n})]^3} \right) \left(\frac{s}{4} - m_{\rho_n}^2 \right) v(s) \log \frac{1+v(s)}{1-v(s)}, \quad (4)$$

$$p(s) = \frac{1}{2}(s - 4m_\pi^2)^{1/2}, \quad v(s) = \sqrt{1 - \frac{4m_\pi^2}{s}}. \quad (5)$$

Correspondingly we use the s -dependent widths

$$\Gamma_{\rho_n}(s) = \frac{m_{\rho_n}^2}{s} \left(\frac{p(s)}{p(m_{\rho_n}^2)} \right)^3 \Gamma_{\rho_n} \theta(s - 4m_\pi^2), \quad (6)$$

which are taken from two-body P -wave final states and for simplicity (and lack of experimental information) also used for the rest of decay channels [32]. In Eqs. (4) and (6) we have used $\Gamma_{\rho_n} \equiv \Gamma_{\rho_n}(s = m_{\rho_n}^2)$, which is the total width of the ρ_n meson. The constraint $\sum_{n=0}^{\infty} c_{\rho_n}^\pi = 1$ together with $\text{BW}_{\rho_n}(0) = 1$ enforces the proper normalization of the form factor $F_\pi(0) = 1$.

For the ground state $\rho(770)$ isospin violation from $\rho - \omega$ mixing is taken into account by substituting

$$c_{\rho_0}^\pi \text{BW}_{\rho_0}(s) \rightarrow \frac{c_{\rho_0}^\pi \text{BW}_{\rho_0}(s)}{1 + c_\omega^\pi} (1 + c_\omega^\pi \text{BW}_\omega). \quad (7)$$

A Breit-Wigner function with constant width

$$\text{BW}_\omega = \frac{m_\omega^2}{m_\omega^2 - s - im_\omega \Gamma_\omega} \quad (8)$$

is used for the description of the ω resonance.

As discussed in the Introduction, the couplings $c_{\rho_n}^\pi$ are based on the ansatz predicted in the dual-QCD $_{N_c=\infty}$ model

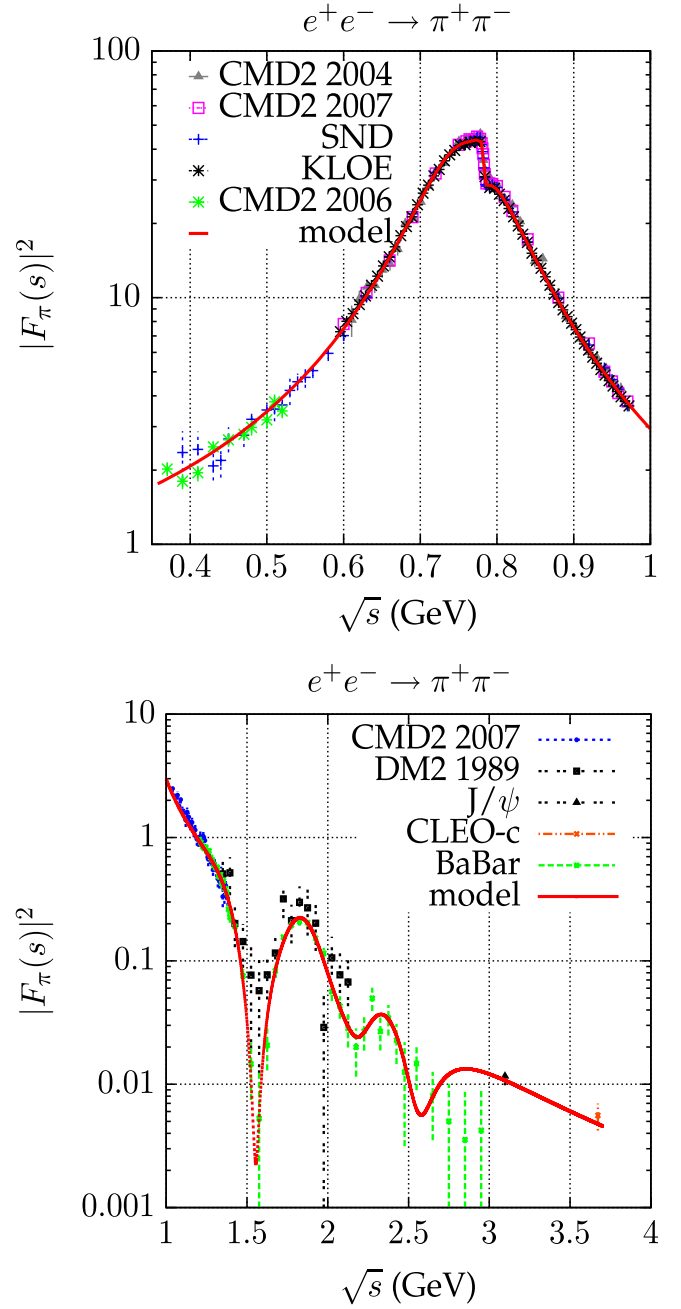


FIG. 1 (color online). The experimental data [3,4,33,36–40,47] compared to the model fits results (see text for details). The form factor at J/ψ comes from its theoretical extraction [31,41] from the data.

[34]

$$c_{\rho_n}^\pi = \frac{(-1)^n \Gamma(\beta - 1/2)}{\alpha' m_{\rho_n}^2 \sqrt{\pi} \Gamma(n+1) \Gamma(\beta - 1 - n)}, \quad (9)$$

where $\alpha' = 1/(2m_{\rho_0}^2)$ is the slope of the Regge trajectory $\alpha_\rho(s) = 1 + \alpha'(s - m_{\rho_0}^2)$. The model postulates an equidistant mass spectrum $m_{\rho_n}^2 = m_{\rho_0}^2(1 + 2n)$ and a linear relation between mass and width of a given resonance

$\Gamma_{\rho_n} = \gamma m_{\rho_n}$, with γ derived from the lowest resonance. The parameters β and m_{ρ_0} are to be taken from the fit.

We fit the data in the timelike region, which provides detailed information about the structure of the resonances and coincides with the region relevant for the PHOKHARA Monte Carlo generator.

We have used new data [3,4,33,36–40] whenever possible. They are more accurate and the treatment of radiative corrections is well documented. Furthermore, we adopt the theoretical extraction of the pion form factor at J/ψ using [31]

$$|F_\pi|^2 = \frac{4B(J/\psi \rightarrow \pi^+\pi^-)}{\beta_\pi^3 B(J/\psi \rightarrow e^+e^-)}, \quad (10)$$

($\beta_\pi = \sqrt{1 - 4m_\pi^2/M_{J/\psi}^2}$), and recent experimental data [41].

If one would assume independent point to point statistical and systematic errors of the new data [3,36–40] and combine these in quadrature, the results would be inconsistent and no fit could be made. Summing linearly the statistical and systematic experimental errors for each experimental data point, one finds very good agreement between the experimental data. This approach will be

TABLE I. Parameters of the pion form factor [Eq. (1) and (11)] and results of the fit to the data.

Parameter	Model (fit)	PDG value [41]	Model
m_{ρ_0}	773.37 ± 0.19	775.49 ± 0.34	input
Γ_{ρ_0}	147.1 ± 1.0	149.4 ± 1.0	input
m_ω	782.4 ± 0.5	782.41 ± 0.12	...
Γ_ω	8.33 ± 0.27	8.49 ± 0.08	...
m_{ρ_1}	1490 ± 11	1465 ± 25	1340
Γ_{ρ_1}	429 ± 27	400 ± 60	256
m_{ρ_2}	1870 ± 25	1720 ± 20	1730
Γ_{ρ_2}	357 ± 46	250 ± 100	330
m_{ρ_3}	2120 [22]	...	2047
Γ_{ρ_3}	300 [22]	...	391
m_{ρ_4}	model	...	2321
Γ_{ρ_4}	model	...	444
m_{ρ_5}	model	...	2567
Γ_{ρ_5}	model	...	491
β	2.148 ± 0.003	...	input
$ c_\omega^\pi $	$(18.7 \pm 0.5) \times 10^{-4}$
$\text{Arg}(c_\omega^\pi)$	0.106 ± 0.020
$ F_2 $	0.59 ± 0.10
$\text{Arg}(F_2)$	-2.20 ± 0.16
$ F_3 $	0.048 ± 0.056
$\text{Arg}(F_3)$	$-2. \pm 1.4$
$ F_4 $	0.40 ± 0.07
$\text{Arg}(F_4)$	-2.9 ± 0.3
$ F_5 $	0.43 ± 0.05
$\text{Arg}(F_5)$	1.19 ± 0.18
$\chi^2/\text{d.o.f.}$	271/270

adopted below. The new *BABAR* data [4] became available only after our analysis was finished, and we include here only their part (above 1.2 GeV). The *BABAR* data below 1.2 GeV are in conflict with KLOE data and further investigations would be required on how to merge these conflicting data samples.

In [3,36–40] the form factor including vacuum polarization was measured. We prefer to parametrize the “bare” form factor F_π (see [25] for definition), which is used throughout this paper and, for example, directly obtained in Eq. (10). The vacuum polarization corrections are taken from [20,42]. For the extraction of the form factor from the cross section, the CLEO-c Collaboration [33] has corrected for the leptonic part of the vacuum polarization effects. Hence their result has still to be corrected only for the hadronic part, which corresponds to a 1.5% shift of $|F_\pi|^2$ only and is irrelevant at the present experimental precision.

We have attempted to fit the experimental data keeping the coupling constants $c_{\rho_n}^\pi$ fixed to the model values (one fit parameter β for all of them) and fitting only the masses and the widths of the first few resonances (up to $n = 5$). This parametrization is satisfactory up to $\sqrt{s} \sim 1.3\text{--}1.4$ GeV, where the details of the model for resonances, with $n = 2$ and higher, are not important. However, the model is definitively too simple for a description of the details of higher radial excitations, including issues like coupled channels in decays of the higher radial ρ excitations. Hence we adopt a heuristic approach, where we allow for arbitrary complex couplings f_n of the ρ_n ($n = 1, 2, 3, 4, 5$)

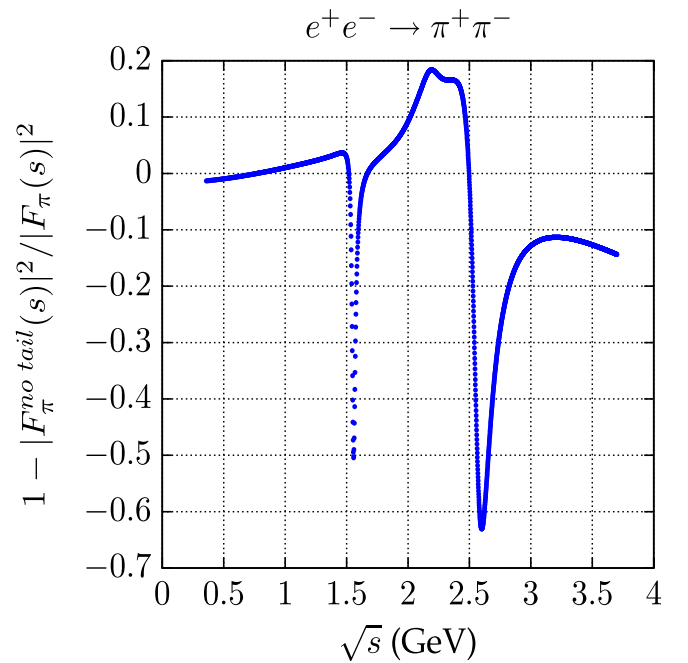


FIG. 2 (color online). The relative difference between the form modulus square of the pion form factor and the form factor calculated with the first six ($N = 0, \dots, 5$) resonances.

$$f_n = F_n \left(\sum_{i=1}^5 c_{\rho_i}^\pi \right) / \left(\sum_{i=1}^5 F_i \right), \quad (11)$$

with $F_1 = 1$ and four complex constants F_n , $n = 2, 3, 4, 5$ fitted to the experimental data.

The mass and the width of ρ_3 are fixed to their values obtained in the fit to the four pion production data [22]. For the masses and widths of the higher excitations ($n \geq 4$) we use their model values.

The results are shown in Table I and Fig. 1. The fitted value of m_{ρ_0} is smaller than its PDG2008 [41] value, a consequence of using the dressed form factor in [36–40]. This phenomenon was also observed in [43]. The parameters describing the radial ρ excitations obtained in the fit have to be taken with great care as they are strongly correlated, while in Table I we give only MINOS (MINUIT procedure from CERNLIB) parabolic errors.

To illustrate the numerical importance of the higher radial excitations within the “dual QCD model” in Fig. 2, we show the relative difference between the full

modulus square of the pion form factor and the result calculated with the first six resonances that were used in the fit. It is evident that it is impossible to neglect the higher resonances and even in the ρ_0 region they give small, but not negligible, contributions to the form factor.

III. THE KAON FORM FACTOR

The kaon form factors were revisited for the same reasons as the pion form factor. Compared to the CLEO-c result [33], the model presented in [32] underestimates the kaon form factor in the vicinity of the $\psi(2S)$ resonance. It is impossible to fit the existing data, including the CLEO-c result, with the functional form used in [32] or by adding one or two more radial excitations, unless one would accept inclusion of a huge wide resonance in the region between J/ψ and $\psi(2S)$. To cure the situation, a model analogous to the one used for the pion form factor, assuming an infinite tower of resonances, was adopted. The ansatz reads

$$F_{K^+}(s) = \frac{1}{2} \left(\left[\sum_{n=0}^{N_\rho} c_{\rho_n}^K \text{BW}_{\rho_n}(s) \right]_{\text{fit}} + \left[\sum_{n=N_\rho+1}^{\infty} c_{\rho_n}^K \text{BW}_{\rho_n}(s) \right]_{d\text{QCD}} \right) + \frac{1}{6} \left(\left[\sum_{n=0}^{N_\omega} c_{\omega_n}^K \text{BW}_{\omega_n}^c(s) \right]_{\text{fit}} + \left[\sum_{n=N_\omega+1}^{\infty} c_{\omega_n}^K \text{BW}_{\omega_n}^c(s) \right]_{d\text{QCD}} \right) + \frac{1}{3} \left(\left[\sum_{n=0}^{N_\phi} c_{\phi_n}^K \text{BW}_{\phi_n}^K(s) \right]_{\text{fit}} + \left[\sum_{n=N_\phi+1}^{\infty} c_{\phi_n}^K \text{BW}_{\phi_n}^K(s) \right]_{d\text{QCD}} \right), \quad (12)$$

$$F_{K^0}(s) = -\frac{1}{2} \left(\left[\sum_{n=0}^{N_\rho} c_{\rho_n}^K \text{BW}_{\rho_n}(s) \right]_{\text{fit}} + \left[\sum_{n=N_\rho+1}^{\infty} c_{\rho_n}^K \text{BW}_{\rho_n}(s) \right]_{d\text{QCD}} \right) + \frac{1}{6} \left(\left[\sum_{n=0}^{N_\omega} c_{\omega_n}^K \text{BW}_{\omega_n}^c(s) \right]_{\text{fit}} + \left[\sum_{n=N_\omega+1}^{\infty} c_{\omega_n}^K \text{BW}_{\omega_n}^c(s) \right]_{d\text{QCD}} \right) + \frac{1}{3} \left(\left[\eta_\phi c_{\phi_0}^K \text{BW}_{\phi_0}^K(s) + \sum_{n=1}^{N_\phi} c_{\phi_n}^K \text{BW}_{\phi_n}^K(s) \right]_{\text{fit}} + \left[\sum_{n=N_\phi+1}^{\infty} c_{\phi_n}^K \text{BW}_{\phi_n}^K(s) \right]_{d\text{QCD}} \right). \quad (13)$$

The couplings in the part with subscript fit were fitted to the experimental data as well as the constants η_ϕ and $c_{\phi_0}^K$. The values of N_ρ , N_ω , and N_ϕ are listed in Table II. The entry PDG in Table II implies that masses and widths as given in PDG2008 [41] were used. The masses and widths of the radial excitations, which were not measured, were calculated assuming an equidistant mass spectrum and a linear relation between the mass and the width of a given resonance

$$m_{j_n}^2 = m_j^2(1 + 2n), \quad \Gamma_{j_n} = \gamma_j m_{j_n}, \quad j = \rho, \omega, \phi. \quad (14)$$

The value of γ_ρ was calculated from Eq. (14) for $n = 0$, and the other values were fitted to the data.

Two versions of the model were investigated: the “unconstrained” version where the couplings between kaons and ρ_n , ω_n , and ϕ_n are not related and the “constrained”

version where $c_{\omega_n}^K = c_{\rho_n}^K$, $n = 0, \dots, \infty$. The constrained model is not able to reproduce data as good as the unconstrained model; however, as is evident from Table II, the corrections to the assumption $c_{\omega_n}^K = c_{\rho_n}^K$ are small for the lowest two resonances.

Despite this, the two models predict completely different asymptotic behavior of the neutral kaon form factor in the region, where no data are available (see Fig. 4 below). The constrained model, being closer to the SU(3) symmetric case where the neutral kaon form factor vanishes, arrives at significantly smaller predictions. The values of the couplings, which were not fitted, were calculated from the formula

$$c_{j_n}^K = \frac{(-1)^n \Gamma(\beta_j^K - 1/2)}{\alpha' \sqrt{\pi} m_{j_n}^2 \Gamma(n+1) \Gamma(\beta_j^K - 1 - n)}, \quad (15)$$

$$\alpha' = 1/(2m_{j_0}^2), \quad j = \rho, \omega, \phi,$$

TABLE II. Parameters of the kaon form factors and results of the fit to the data. Masses and widths are given in MeV. The column Fit (1) [Fit(2)] contains the values of the constrained (unconstrained) fits.

Parameter	Input	Fit(1)	Fit(2)	PDG value	Model(1)	Model(2)
m_{ϕ_0}	...	1019.415 ± 0.004	1019.415 ± 0.003	1019.455 ± 0.020	input	input
Γ_{ϕ_0}	...	4.34 ± 0.01	4.22 ± 0.04	4.26 ± 0.05	input	input
m_{ϕ_1}	1680	1680 ± 20	1766	1766
Γ_{ϕ_1}	150	150 ± 50	353	353
m_{ρ_0}	775.49	775.49 ± 0.34	input	input
Γ_{ρ_0}	149.4	149.4 ± 1.0	input	input
m_{ρ_1}	1465	1465 ± 25	1345	1345
Γ_{ρ_1}	400	400 ± 60	259	259
m_{ρ_2}	...	1680 ± 4	PDG	1720 ± 20	1734	1734
Γ_{ρ_2}	...	365 ± 59	PDG	250 ± 100	334	334
m_{ω_0}	782.65	782.65 ± 0.12	input	input
Γ_{ω_0}	8.49	8.49 ± 0.08	input	input
m_{ω_1}	1425	1400–1450	1356	1356
Γ_{ω_1}	...	145 ± 9	PDG	180–250	678	678
m_{ω_2}	...	1729 ± 76	PDG	1670 ± 30	1750	1750
Γ_{ω_2}	...	245 ± 9	PDG	315 ± 35	875	875
η_ϕ	...	1.040 ± 0.007	1.055 ± 0.010
β_ϕ	$c_{\phi_0}^K$ (15)	1.97 ± 0.02	1.91 ± 0.02
γ_ϕ	...	0.2	0.2	...	input	input
$c_{\phi_0}^K$...	0.985 ± 0.006	0.947 ± 0.009	...	input	input
$c_{\phi_1}^K$...	0.0042 ± 0.0015	0.0136 ± 0.0024	...	0.0084	0.0271
$c_{\phi_2}^K$...	0.0039 ± 0.0026	(16) 0.0214 ± 0.0093	...	0.0026	0.0088
$c_{\phi_3}^K$...	(16) 0.0033 ± 0.0067	0.0012	...
$\sum_{n=N_\phi+1}^{\infty} c_{\phi_n}^K$	model	0.0036	0.0180	...	0.0036	0.0180
β_ρ	$c_{\rho_0}^K$ (15)	2.23 ± 0.06	2.21 ± 0.05
γ_ρ	...	0.193 (14) ($= \Gamma_\rho/m_\rho$)	0.193 (14) ($= \Gamma_\rho/m_\rho$)	...	input	input
$c_{\rho_0}^K$...	1.138 ± 0.011	1.120 ± 0.007	...	input	input
$c_{\rho_1}^K$...	-0.043 ± 0.014	-0.107 ± 0.010	...	-0.087	-0.078
$c_{\rho_2}^K$...	-0.144 ± 0.015	-0.028 ± 0.012	...	-0.020	-0.019
$c_{\rho_3}^K$...	-0.004 ± 0.007	(16) 0.032 ± 0.017	...	-0.0084	-0.0079
$c_{\rho_4}^K$...	(16) 0.0662 ± 0.0243	-0.0045	...
$\sum_{n=N_\rho+1}^{\infty} c_{\rho_n}^K$	model	-0.0132	-0.0170	...	-0.0132	-0.0170
β_ω	$c_{\omega_0}^K$ (15)	β_ρ	2.75 ± 0.06
γ_ω	...	0.5	0.5	...	input	input
$c_{\omega_0}^K$...	$c_{\rho_0}^K$	1.37 ± 0.03	...	input	input
$c_{\omega_1}^K$...	$c_{\rho_1}^K$	-0.173 ± 0.003	...	-0.087	-0.345
$c_{\omega_2}^K$...	$c_{\rho_2}^K$	-0.621 ± 0.020	...	-0.020	-0.026
$c_{\omega_3}^K$...	$c_{\rho_3}^K$	(16) 0.43 ± 0.04	...	-0.0084	-0.0079
$c_{\omega_4}^K$...	$c_{\rho_4}^K$	-0.0045	...
$\sum_{n=N_\omega+1}^{\infty} c_{\omega_n}^K$	model	$\sum_{n=N_\rho+1}^{\infty} c_{\rho_n}^K$	-0.0096	...	-0.0132	-0.0096
$\chi^2/\text{d.o.f.}$...	277/256	221/260

with the exception of the couplings next to the last fitted, which were calculated from the normalization requirements

$$\sum_{n=0}^{\infty} c_{j_n}^K = 1, \quad j = \rho, \omega, \phi. \quad (16)$$

Breit-Wigner propagators

$$\text{BW}_\alpha^c = \frac{m_\alpha^2}{m_\alpha^2 - s - im_\alpha \Gamma_\alpha}, \quad \alpha = \omega_n, \quad (17)$$

with constant widths were used for all ω_n , Breit-Wigner propagators with s -dependent widths

$$\text{BW}_{\phi_n}^j = \frac{m_{\phi_n}^2}{m_{\phi_n}^2 - s - im_{\phi_n} \Gamma_{\phi_n}^j}, \quad (18)$$

$$\Gamma_{\phi_n}^j = \frac{m_{\phi_n}^2}{s} \left(\frac{s - 4m_j^2}{m_{\phi_n}^2 - 4m_j^2} \right)^{3/2} \Gamma_{\phi_n}, \quad j = K^+, K^0,$$

were used for ϕ_n , the radial excitations of ϕ , and the GS Breit-Wigner functions [Eq. (2)] were used for ρ_n . The

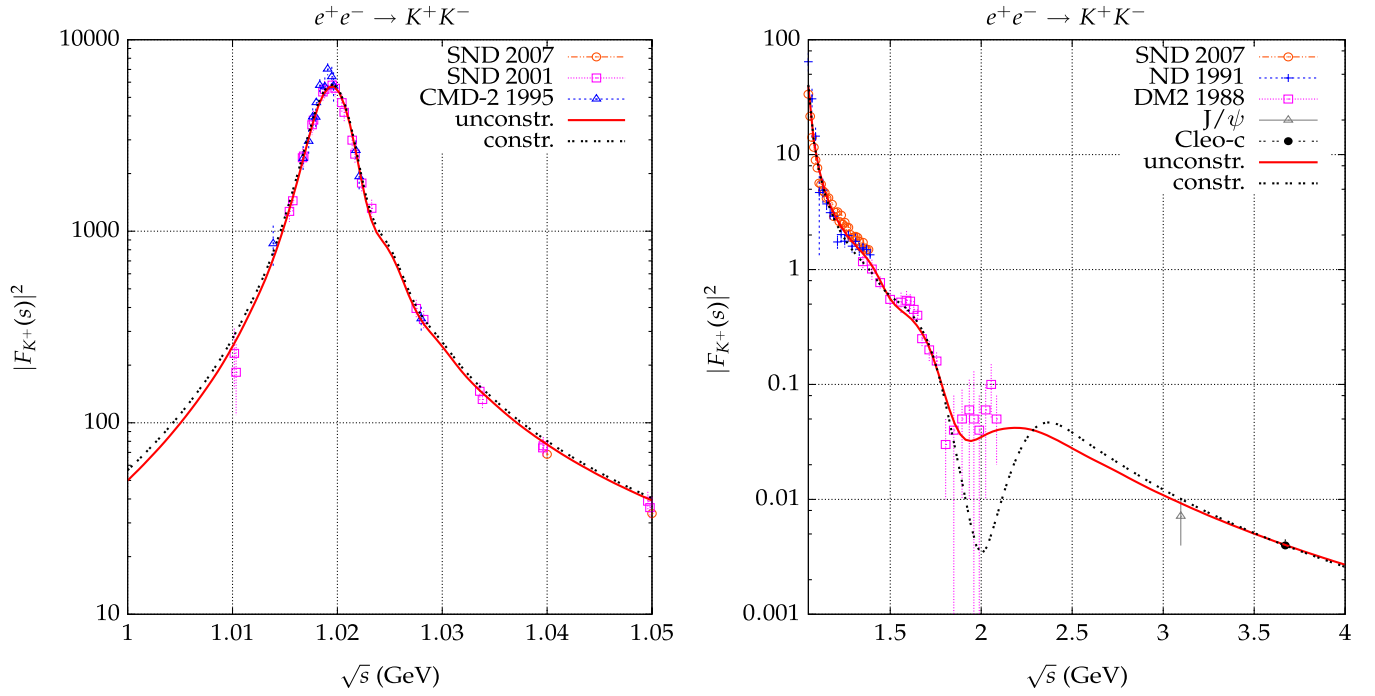


FIG. 3 (color online). The experimental data [33,48–52] compared to the model fits results (see text for details). The form factor at J/ψ comes from its theoretical extraction [26] from the data. It was not used in the fit.

parameters β_j^K , $j = \rho$, ω , and ϕ were calculated from Eq. (15) using the fitted $c_{j_0}^K$ parameter. The results of the fits are summarized in Table II and in Figs. 3 and 4. The high energy behavior of both form factors is completely driven by the CLEO [33] measurement.

Following [32], i.e. assuming isospin symmetry, one arrives at the following predictions for the branching ratio of the τ -lepton decay into $K^- K^0 \nu_\tau$:

$$\text{Br}(\tau^- \rightarrow K^- K^0 \nu_\tau) = (0.135/0.190) \cdot 10^{-3} \quad (19)$$

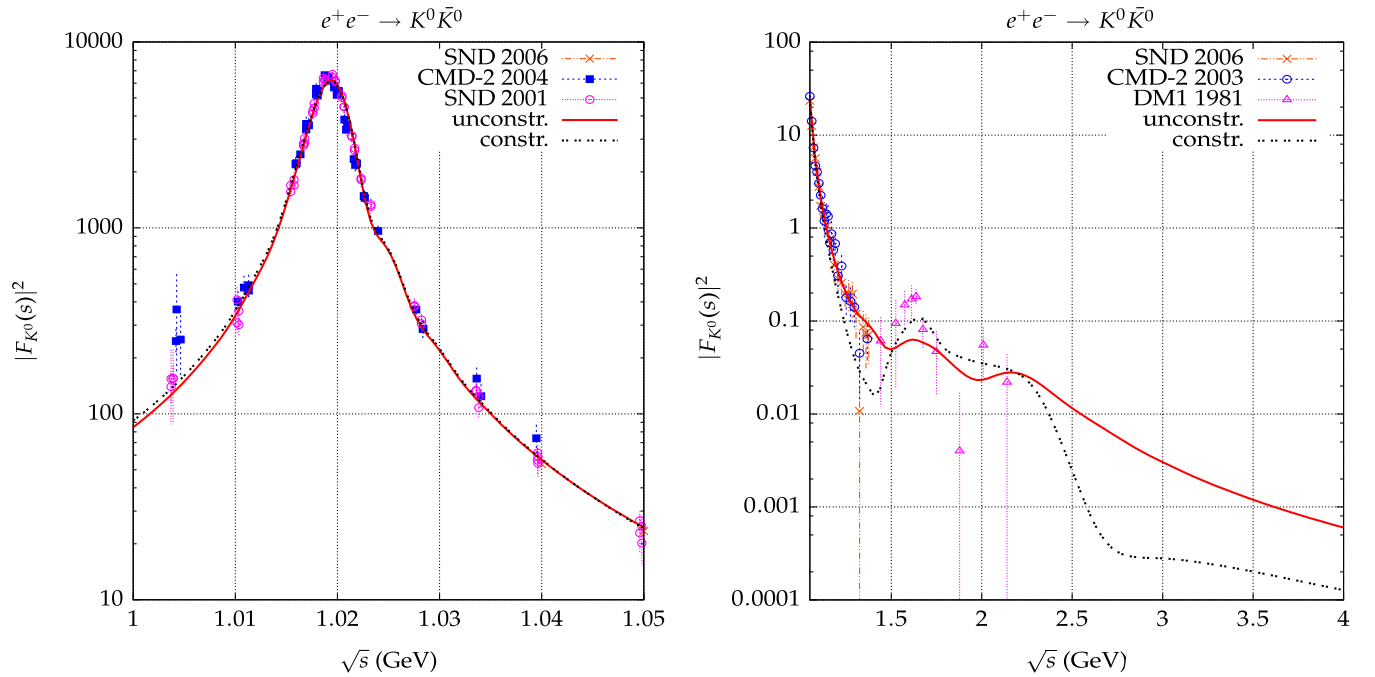


FIG. 4 (color online). The experimental data [40,48,53–55] compared to the model fits results (see text for details).

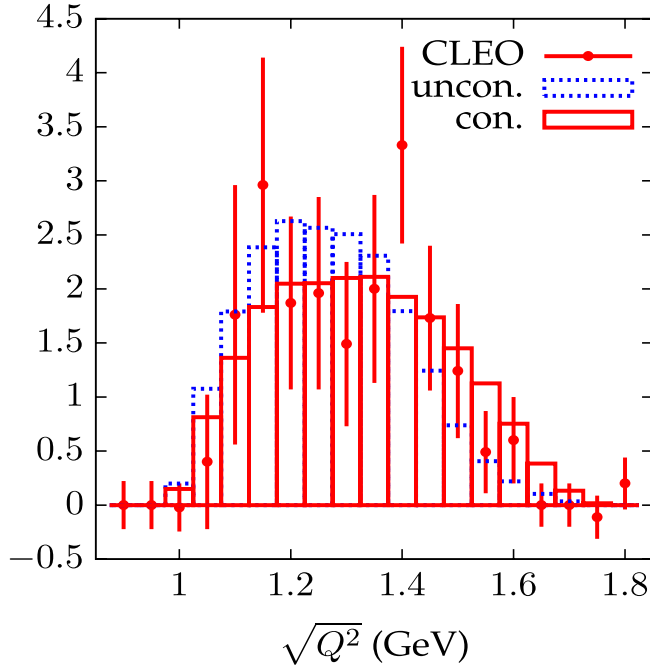


FIG. 5 (color online). Normalized distributions $\frac{d\Gamma(\tau \rightarrow K^- K^0 \nu_\tau)/d\sqrt{Q^2}}{\Gamma(\tau \rightarrow K^- K^0 \nu_\tau)}$ of the kaon pair invariant mass predicted within two models, described in the text. CLEO data [44] normalized to the total number of events are also shown.

for unconstrained and constrained models, respectively. The model dependence is characterized by the spread between the two results and is far larger than the errors resulting from the fits of the parameters within one model. These results can be compared with the PDG value [41]

$$\text{Br}(\tau^- \rightarrow K^- K^0 \nu_\tau) = (0.158 \pm 0.16) \cdot 10^{-3} \quad (20)$$

and are found to be reasonably consistent.

Within the same assumptions one can predict the $K^- K^0$ invariant mass distribution and compare it (see Fig. 5) with existing CLEO data [44]. As evident from Fig. 5 both models give very similar predictions and both agree with the data. Thus we conclude that within the current experimental accuracy, which is, however, very poor, isospin symmetry works well and the details of the models do not play any role in its tests.

IV. MONTE CARLO IMPLEMENTATION OF $K^+ K^-$ AND $K^0 \bar{K}^0$

The event generator PHOKHARA has been extended to generate $K^+ K^-$ and $K^0 \bar{K}^0$ final states. In this section we present the implementation and results for the region below the narrow resonances J/ψ and $\psi(2S)$. Charged kaons have been implemented in the same way as the $\pi^+ \pi^-$ channel [15,16], with the kaon form factor described in Sec. III. The NLO FSR corrections have been implemented

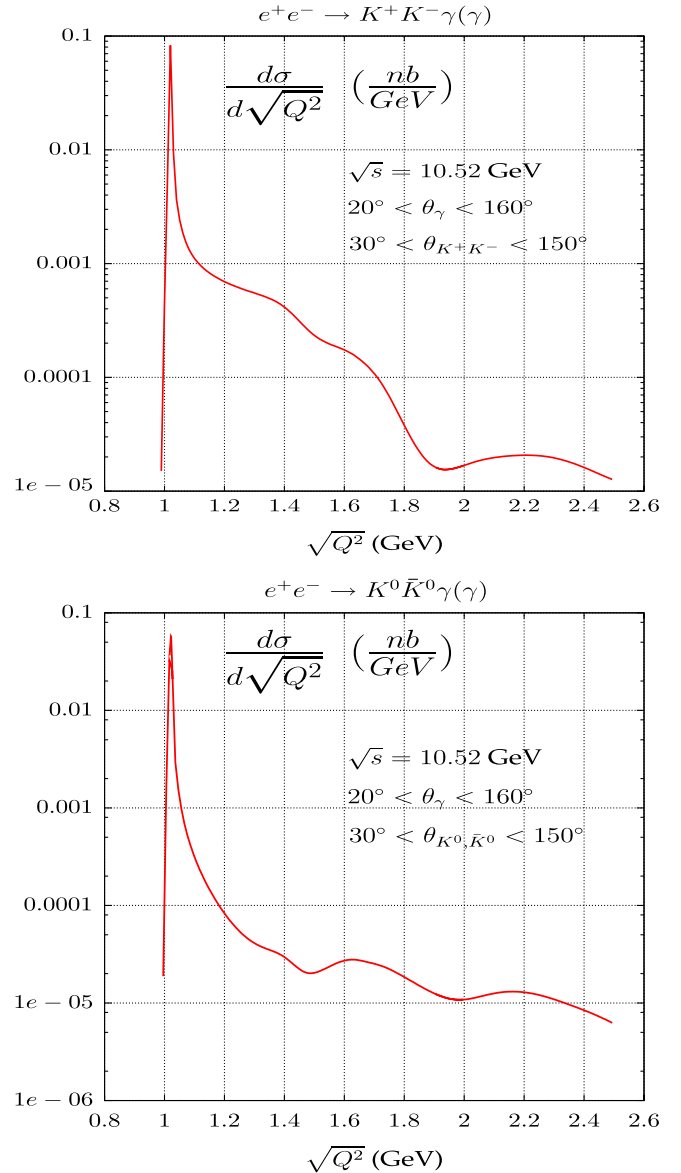


FIG. 6 (color online). Differential cross section for $\sqrt{s} = 10.52$ GeV of the processes $e^+e^- \rightarrow K^+K^-\gamma(\gamma)$ and $e^+e^- \rightarrow K^0\bar{K}^0\gamma(\gamma)$ with angular cuts.

as well. For the neutral kaons the corrections are limited to ISR. With the enormous luminosity of B factories one expects hundreds of events even for Q^2 between 3 and 4 GeV^2 and large statistics around the ϕ resonance (Fig. 6). The next-to-leading FSR corrections are relevant for a measurement in the neighborhood of the ϕ resonance if an accuracy better than 10% is aimed (Fig. 7).

V. NARROW RESONANCES AND THE RADIATIVE RETURN

The radiative return, as implemented now in PHOKHARA, receives contributions from a multitude of amplitudes

shown in Fig. 8. The notation introduced in this figure also applies to the narrow resonance amplitudes. Below we list the formulas for $\mu^+\mu^-$, $\pi^+\pi^-$, K^+K^- , and \bar{K}^0K^0 . For the \bar{K}^0K^0 amplitude FSR emission is not present. We explicitly

indicate the vacuum polarization contributions as well as the ϕ contribution. We assume that in the vacuum polarization J/ψ , $\psi(2S)$ and ϕ were not accounted for. The differential cross section given by PHOKHARA reads

$$\begin{aligned}
 d\sigma = & |M_{\gamma_1, \text{LOISR}} \cdot C_{R,P}^{VP}(Q^2) + M_{\gamma_1, \text{LOFSR}} \cdot C_{R,P}^{VP}(s)|^2 d\Phi_1 + |M_{2\gamma, \text{ISR}} \cdot C_{R,P}^{VP}(Q^2)|^2 d\Phi_2 + 2 \text{Re}(M_{\gamma_1, \text{NLOISR}} \times M_{\gamma_1, \text{LOISR}}^\dagger) \\
 & \cdot |C_{R,P}^{VP}(Q^2)|^2 d\Phi_1 + |M_{\gamma_1, \text{ISR}; \gamma, \text{FSR}} \cdot C_{R,P}^{VP}((Q + k_\gamma)^2)|^2 d\Phi_2 + 2 \text{Re}(M_{\gamma_1, \text{LOFSR}}^{\text{NLOFSR}} \times M_{\gamma_1, \text{LOISR}}^\dagger) \cdot |C_{R,P}^{VP}(Q^2)|^2 d\Phi_1 \\
 & + |M_{\gamma_1, \text{ISR}; \gamma_1, \text{FSR}} \cdot C_{R,P}^{VP}((Q + k_{\gamma_1})^2)|^2 d\Phi_2 + 2 \text{Re}(M_{\gamma_1, \text{LOFSR}}^{\text{NLOISR}} \times M_{\gamma_1, \text{LOFSR}}^\dagger) \cdot |C_{R,P}^{VP}(s)|^2 d\Phi_1,
 \end{aligned} \quad (21)$$

where

$$\begin{aligned}
 C_{R,P}^{VP}(s) = & \frac{1}{1 - \Delta\alpha(s)} - \frac{3\Gamma_e^\phi}{\alpha m_\phi} \text{BW}_\phi(s) \delta_P + C_{J/\psi, P}(s) \\
 & + C_{\psi(2S), P}(s),
 \end{aligned} \quad (22)$$

$$C_{R,P}(s) = \frac{3\sqrt{s}}{\alpha} \frac{\Gamma_e^R(1 + c_P^R)}{s - M_R^2 + i\Gamma_R M_R}, \quad (23)$$

and $d\Phi_1$ ($d\Phi_2$) denote the phase space with one (two) photon(s) in the final state with all statistical factors included.

For $P = \mu$ and $P = \pi$, $c_P^R = 0$ (no direct decay of the narrow resonances into $\mu^+\mu^-$ and $\pi^+\pi^-$), while $\delta_P = 0$ for $P = K$ and $\delta_P = 1$ for $P = \mu$ and $P = \pi$. The ϕ contributions to the kaon pair production are included in the kaon form factor, hence $\delta_K = 0$. The notation and the detailed description of the narrow resonance contribution to the amplitude can be found in [25] (see [27] for similar

studies). From [25] we also take $|c_{K^+}^{J/\psi}| = 1.27 \pm 0.32$ and $|c_{K^+}^{\psi(2S)}| = 2.94 \pm 0.99$. The information on the neutral kaon couplings to the narrow resonances is almost non-existing, and we use the lower limits of $|c_{K^0}^{J/\psi}| = 2.81$, $|c_{K^0}^{\psi(2S)}| = 5.35$, which correspond to the upper limit on the neutral kaon form factor (see [25] for details). The phases are essentially not known, and we use 100° to obtain the numerical values in the next section.

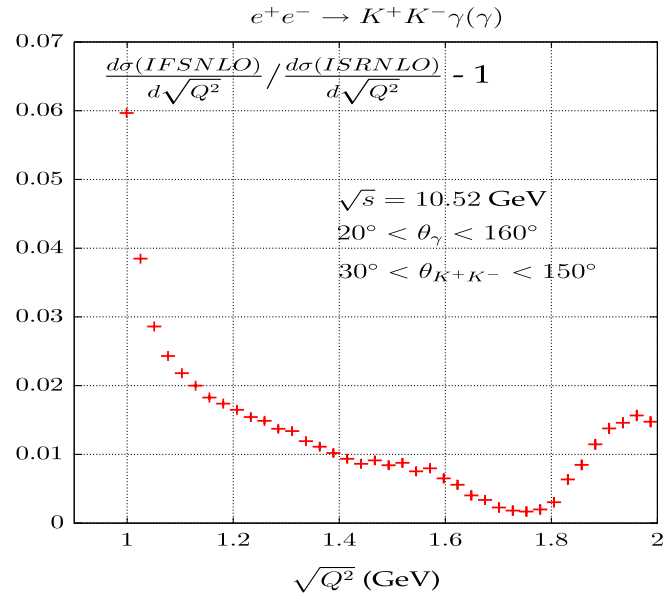


FIG. 7 (color online). Comparison of IFSNLO and ISRNLO distributions with angular cuts.

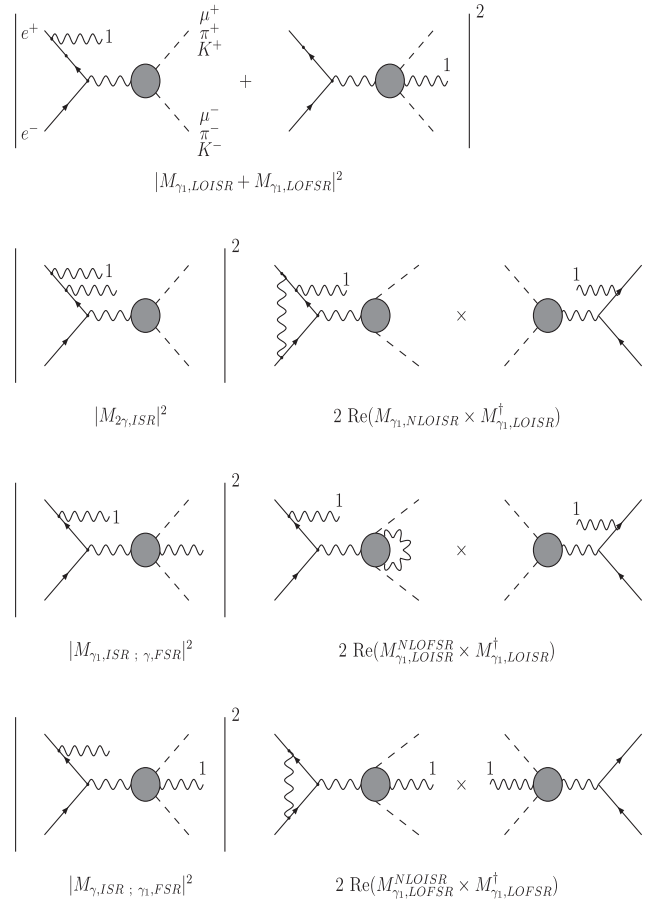


FIG. 8. The contributions to the radiative return cross section included in PHOKHARA. Label “1” at a photon line means that the photon is hard.

VI. THE IMPLEMENTATION OF NARROW RESONANCES INTO THE MONTE CARLO EVENT GENERATOR PHOKHARA

The tests of the ISR part of the implementation of the narrow resonances were straightforward and followed the standard tests we perform for each new channel [14–20,22]. The comparisons were made with the analytic formulas of [45] separately for one and two photon emissions. The precision of the comparisons was at the level of a small fraction of a per mill, proving the technical precision of the program at that level. The independence of the results on the separation parameter between soft photon, calculated analytically, and hard photon, generated by means of the Monte Carlo method, was also tested with that precision.

The implementation of the NLO FSR part is more tricky. The analytic formulas used in [16,18] for soft photon contributions are still valid, which we have checked numerically with the precision of 0.02%. However, if one chooses the separation parameter between soft and hard parts at the usual value $w = 10^{-4}$, which corresponds to the photon energy $E_\gamma = 1$ MeV for $\sqrt{s} = 10$ GeV, the “soft” integral receives contributions from the whole resonance region, as a consequence of the small width ($\Gamma_{J/\psi} = 93.4$ keV). For a cutoff of 10^{-4} the part of the matrix element that multiplies the soft emission factor is rapidly varying, and the basic assumption underlying the whole approach, that the soft emission can be integrated analytically with the multiplicative remainder being constant, is no longer valid. Pushing the value of the cutoff to an extremely small value, say 10^{-7} , solves this problem. However, single-photon emission is not an adequate description for such soft photons and in principle one should use exponentiation. From the technical side this is reflected in the appearance of negative weights. Inclusion of Yennie-Frautschi-Suura [46]-like multiphoton production would allow one to cure this problem. However, since this would amount to completely restructuring our Monte Carlo generator, we have adopted a simpler approach, which gives correct distributions, when convoluted with an energy resolution typical for a detector at a ϕ - or B -meson factory.

Because of the finite detector resolution one never observes the true distribution of the events, but the one convoluted with the detector resolution function. This increase of the effective width by about a factor of 100 is sufficient to cure the problem. For a cutoff of 10^{-4} the distribution remains smooth and we can produce the unweighted events sample. The result will, as expected, depend on the resolution of the detector. To check whether this is true for the realistic energy resolution of the *BABAR* detector [24] of 14.5 MeV, we have compared the muon invariant mass distributions obtained with $w = 10^{-4}$ and $w = 10^{-7}$, smeared with a Gaussian distribution with a standard deviation of 14.5 MeV. Even if the nonsmeared distributions are completely different, as shown in Fig. 9,

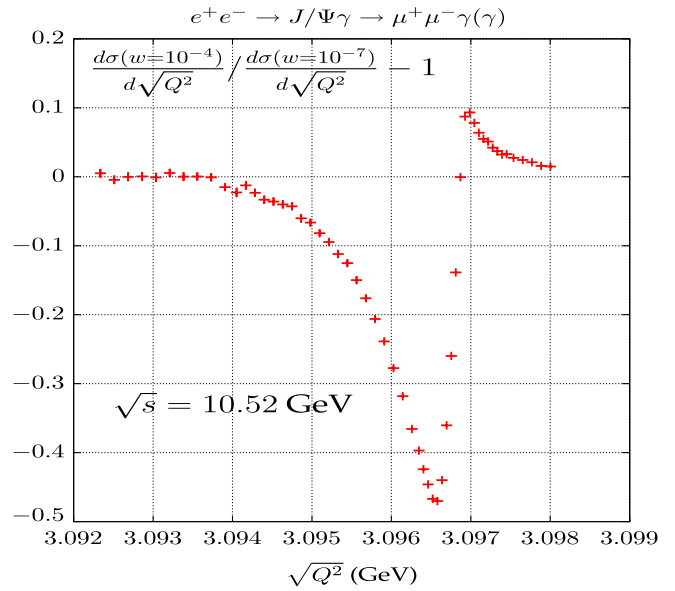


FIG. 9 (color online). Comparison between invariant mass distributions obtained with $w = 10^{-4}$ and $w = 10^{-7}$.

the smeared distributions agree within 2 per mill as shown in Fig. 10. This 2 per mill is the intrinsic error coming from the method we use, but the generator should be accurate enough for any practical purposes.

It is interesting to observe (Fig. 11) that the FSRNLO contributions fill completely the interference dip, still visible if only ISR corrections are taken into account. Thus the absence of the dip in the observed invariant mass distribution is not the only effect of the detector smearing.

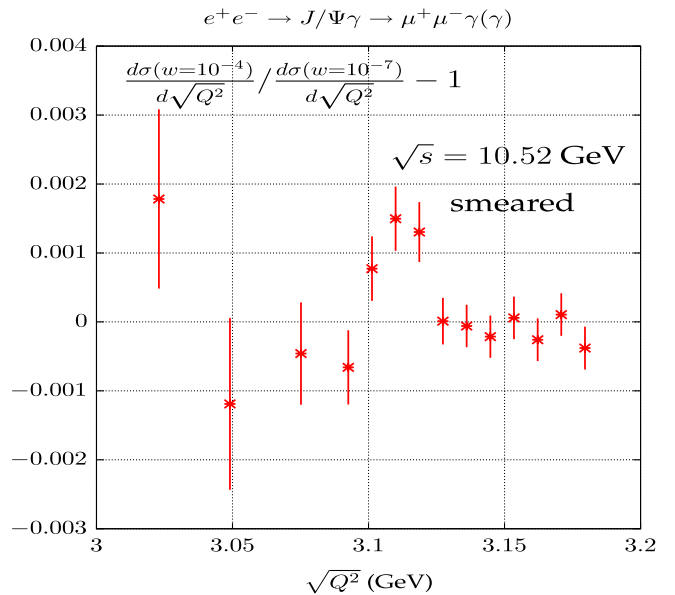


FIG. 10 (color online). Comparison between invariant mass distributions obtained with $w = 10^{-4}$ and $w = 10^{-7}$ smeared with Gaussian with the standard deviation of 14.5 MeV.

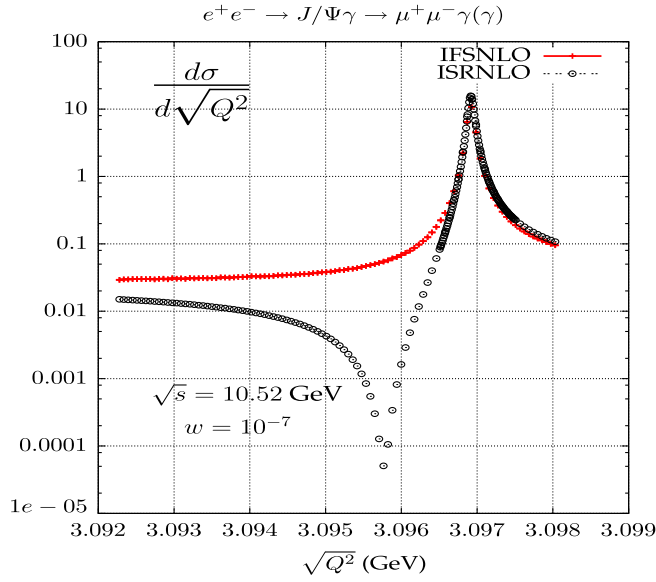


FIG. 11 (color online). Comparisons of the invariant mass distributions obtained with $w = 10^{-7}$ taking into account only ISRNLO contributions and the complete (ISR + FSR)NLO result.

The huge FSRNLO corrections seen in Fig. 11 are washed out if one looks at the detector smeared distributions shown in Fig. 12. The corrections are seen more accurately in Fig. 13, where the relative difference is shown. The FSRNLO corrections cannot be neglected if one aims at a precision better than 10%, unless one considers only the integral over the whole resonance region (together with the sidebands as shown in Fig. 12). In the

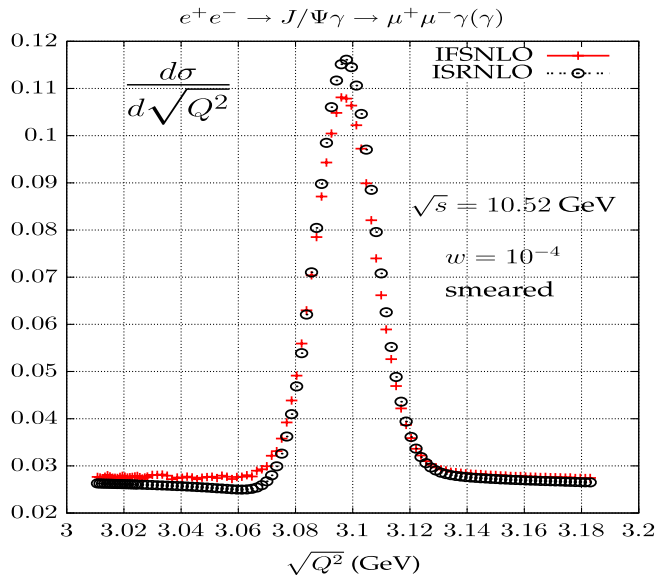


FIG. 12 (color online). Comparisons of the invariant mass distributions obtained with $w = 10^{-7}$ taking into account only ISRNLO contributions and the complete (ISR + FSR)NLO result. Detector smearing effects are taken into account.

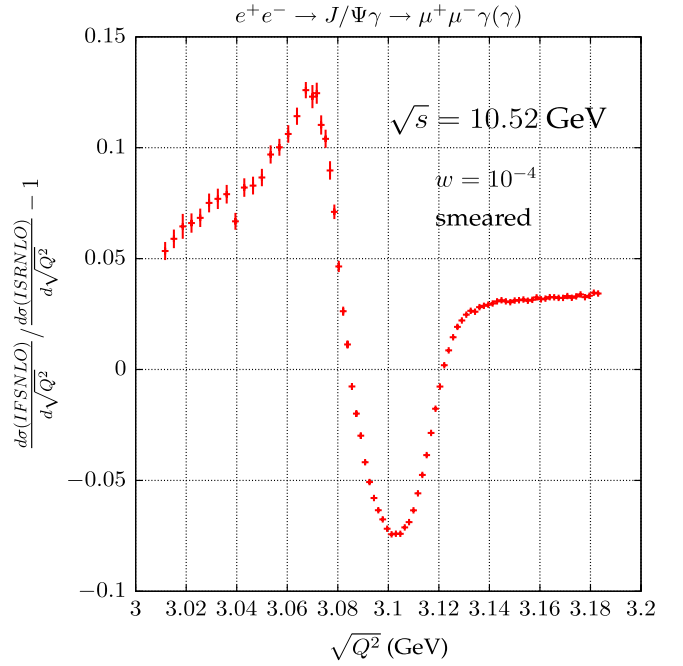


FIG. 13 (color online). Relative ratio of the invariant mass distributions taking into account only ISRNLO contributions and the complete (ISR + FSR)NLO result. Detector smearing effects are taken into account.

integrated cross section a large part of the corrections cancel ($\sigma_{\text{ISRNLO}} = 6.901$ pb, $\sigma_{\text{IFSNLO}} = 6.954$ pb).

Identical tests were performed for the pion pair production with identical conclusions, so we do not present them here.

VII. SUMMARY

New parametrizations of the pion and kaon form factors, based on the “dual QCD model,” are presented, which are derived from a fit to a combination of old measurements and more recent experimental results in the energy region above the ρ resonance. These form factors and the results of a recent analysis of the direct hadronic coupling of $K\bar{K}$ to J/ψ and $\psi(2S)$ are incorporated in the Monte Carlo generator PHOKHARA, which is now also adapted to the simulation of narrow resonances, including the effects of ISR and FSR in NLO.

ACKNOWLEDGMENTS

This work was supported in part by BMBF under Grant No. 05H09VKE, EU 6th Framework Programme under Contract No. MRTN-CT-2006-035482 (FLAVIANet), and EU Research Programmes at LNF, FP7, Transnational Access to Research Infrastructure (TARI), Hadron Physics2-Integrating Activity, Contract No. 227431. Henryk Czyż is grateful for the support and the kind hospitality of the Institut für Theoretische Teilchenphysik of the Karlsruhe Institute of Technology.

- [1] Min-Shih Chen and P.M. Zerwas, *Phys. Rev. D* **11**, 58 (1975).
- [2] S. Binner, J. H. Kühn, and K. Melnikov, *Phys. Lett. B* **459**, 279 (1999).
- [3] F. Ambrosino *et al.* (KLOE Collaboration), *Phys. Lett. B* **670**, 285 (2009).
- [4] B. Aubert *et al.* (BABAR Collaboration), *Phys. Rev. Lett.* **103**, 231801 (2009).
- [5] B. Aubert *et al.* (BABAR Collaboration), *Phys. Rev. D* **73**, 012005 (2006).
- [6] B. Aubert *et al.* (BABAR Collaboration), *Phys. Rev. D* **76**, 092006 (2007).
- [7] B. Aubert *et al.* (BABAR Collaboration), *Phys. Rev. D* **70**, 072004 (2004).
- [8] B. Aubert *et al.* (BABAR Collaboration), *Phys. Rev. D* **77**, 092002 (2008).
- [9] B. Aubert *et al.* (BABAR Collaboration), *Phys. Rev. D* **71**, 052001 (2005).
- [10] B. Aubert *et al.* (BABAR Collaboration), *Phys. Rev. D* **76**, 012008 (2007).
- [11] H. Czyż and J. H. Kühn, *Eur. Phys. J. C* **18**, 497 (2001).
- [12] G. Rodrigo, A. Gehrmann-De Ridder, M. Guillaume, and J. H. Kühn, *Eur. Phys. J. C* **22**, 81 (2001).
- [13] J. H. Kühn and G. Rodrigo, *Eur. Phys. J. C* **25**, 215 (2002).
- [14] G. Rodrigo, H. Czyż, J. H. Kühn, and M. Szopa, *Eur. Phys. J. C* **24**, 71 (2002).
- [15] H. Czyż, A. Grzeźlińska, J. H. Kühn, and G. Rodrigo, *Eur. Phys. J. C* **27**, 563 (2003).
- [16] H. Czyż, A. Grzeźlińska, J. H. Kühn, and G. Rodrigo, *Eur. Phys. J. C* **33**, 333 (2004).
- [17] H. Czyż, J. H. Kühn, E. Nowak, and G. Rodrigo, *Eur. Phys. J. C* **35**, 527 (2004).
- [18] H. Czyż, A. Grzeźlińska, J. H. Kühn, and G. Rodrigo, *Eur. Phys. J. C* **39**, 411 (2005).
- [19] H. Czyż, A. Grzeźlińska, and J. H. Kühn, *Phys. Lett. B* **611**, 116 (2005).
- [20] H. Czyż, A. Grzeźlińska, J. H. Kühn, and G. Rodrigo, *Eur. Phys. J. C* **47**, 617 (2006).
- [21] H. Czyż, A. Grzeźlińska, and J. H. Kühn, *Phys. Rev. D* **75**, 074026 (2007).
- [22] H. Czyż, J. H. Kühn, and A. Wapienik, *Phys. Rev. D* **77**, 114005 (2008).
- [23] S. Actis *et al.*, *Eur. Phys. J. C* **66**, 585 (2010).
- [24] B. Aubert *et al.* (BABAR Collaboration), *Phys. Rev. D* **69**, 011103 (2004).
- [25] H. Czyż and J. H. Kühn, *Phys. Rev. D* **80**, 034035 (2009).
- [26] K. K. Seth, *Phys. Rev. D* **75**, 017301 (2007).
- [27] C. Z. Yuan, P. Wang, and X. H. Mo, *Phys. Lett. B* **567**, 73 (2003).
- [28] J. L. Rosner, *Phys. Rev. D* **60**, 074029 (1999).
- [29] M. Suzuki, *Phys. Rev. D* **60**, 051501(R) (1999).
- [30] G. Lopez Castro, J. L. M. Lucio, and J. Pestieau, *AIP Conf. Proc.* **342**, 441 (1995).
- [31] J. Milana, S. Nussinov, and M. G. Olsson, *Phys. Rev. Lett.* **71**, 2533 (1993).
- [32] C. Bruch, A. Khodjamirian, and J. H. Kühn, *Eur. Phys. J. C* **39**, 41 (2005).
- [33] T. K. Pedlar *et al.* (CLEO Collaboration), *Phys. Rev. Lett.* **95**, 261803 (2005).
- [34] C. A. Dominguez, *Phys. Lett. B* **512**, 331 (2001).
- [35] G. J. Gounaris and J. J. Sakurai, *Phys. Rev. Lett.* **21**, 244 (1968).
- [36] R. R. Akhmetshin *et al.* (CMD-2 Collaboration), *Phys. Lett. B* **648**, 28 (2007).
- [37] R. R. Akhmetshin *et al.*, *Pis'ma Zh. Eksp. Teor. Fiz.* **84**, 491 (2006) [*JETP Lett.* **84**, 413 (2006)].
- [38] M. N. Achasov *et al.*, *Zh. Eksp. Teor. Fiz.* **101**, 1201 (2005) [*J. Exp. Theor. Phys.* **101**, 1053 (2005)].
- [39] V. M. Aulchenko *et al.* (CMD-2 Collaboration), *Pis'ma Zh. Eksp. Teor. Fiz.* **82**, 841 (2005) [*JETP Lett.* **82**, 743 (2005)].
- [40] R. R. Akhmetshin *et al.* (CMD-2 Collaboration), *Phys. Lett. B* **578**, 285 (2004).
- [41] C. Amsler *et al.* (Particle Data Group), *Phys. Lett. B* **667**, 1 (2008).
- [42] F. Jegerlehner, <http://www-zeuthen.desy.de/~fjeger/alphaQED.uu> now at <http://www-com.physik.hu-berlin.de/~fjeger/alphaQED.uu>. The code was changed in the vicinity of the narrow resonances as described in <http://ific.uv.es/~rodrigo/phokhara/phokhara5.0.ps>.
- [43] S. Ghozzi and F. Jegerlehner, *Phys. Lett. B* **583**, 222 (2004).
- [44] T. E. Coan *et al.* (CLEO Collaboration), *Phys. Rev. D* **53**, 6037 (1996).
- [45] F. A. Berends, W. L. van Neerven, and G. J. H. Burgers, *Nucl. Phys.* **B297**, 429 (1988); **B304**, 921(E) (1988).
- [46] D. R. Yennie, S. C. Frautschi, and H. Suura, *Ann. Phys. (N.Y.)* **13**, 379 (1961).
- [47] D. Bisello *et al.* (DM2 Collaboration), *Phys. Lett. B* **220**, 321 (1989).
- [48] M. N. Achasov *et al.*, *Phys. Rev. D* **63**, 072002 (2001).
- [49] R. R. Akhmetshin *et al.*, *Phys. Lett. B* **364**, 199 (1995).
- [50] S. I. Dolinsky *et al.*, *Phys. Rep.* **202**, 99 (1991).
- [51] D. Bisello *et al.* (DM2 Collaboration), *Z. Phys. C* **39**, 13 (1988).
- [52] M. N. Achasov *et al.*, *Phys. Rev. D* **76**, 072012 (2007).
- [53] R. R. Akhmetshin *et al.*, *Phys. Lett. B* **551**, 27 (2003).
- [54] F. Mane, D. Bisello, J. C. Bizot, J. Buon, A. Cordier, and B. Delcourt, *Phys. Lett. B* **99**, 261 (1981).
- [55] M. N. Achasov *et al.*, *Zh. Eksp. Teor. Fiz.* **103**, 831 (2006) [*J. Exp. Theor. Phys.* **103**, 720 (2006)].